

THE OFFICIAL MAGAZINE OF THE OCEANOGRAPHY SOCIETY

Oceanography

CITATION

Socolofsky, S.A., E.E. Adams, C.B. Paris, and D. Yang. 2016. How do oil, gas, and water interact near a subsea blowout? *Oceanography* 29(3):64–75, <http://dx.doi.org/10.5670/oceanog.2016.63>.

DOI

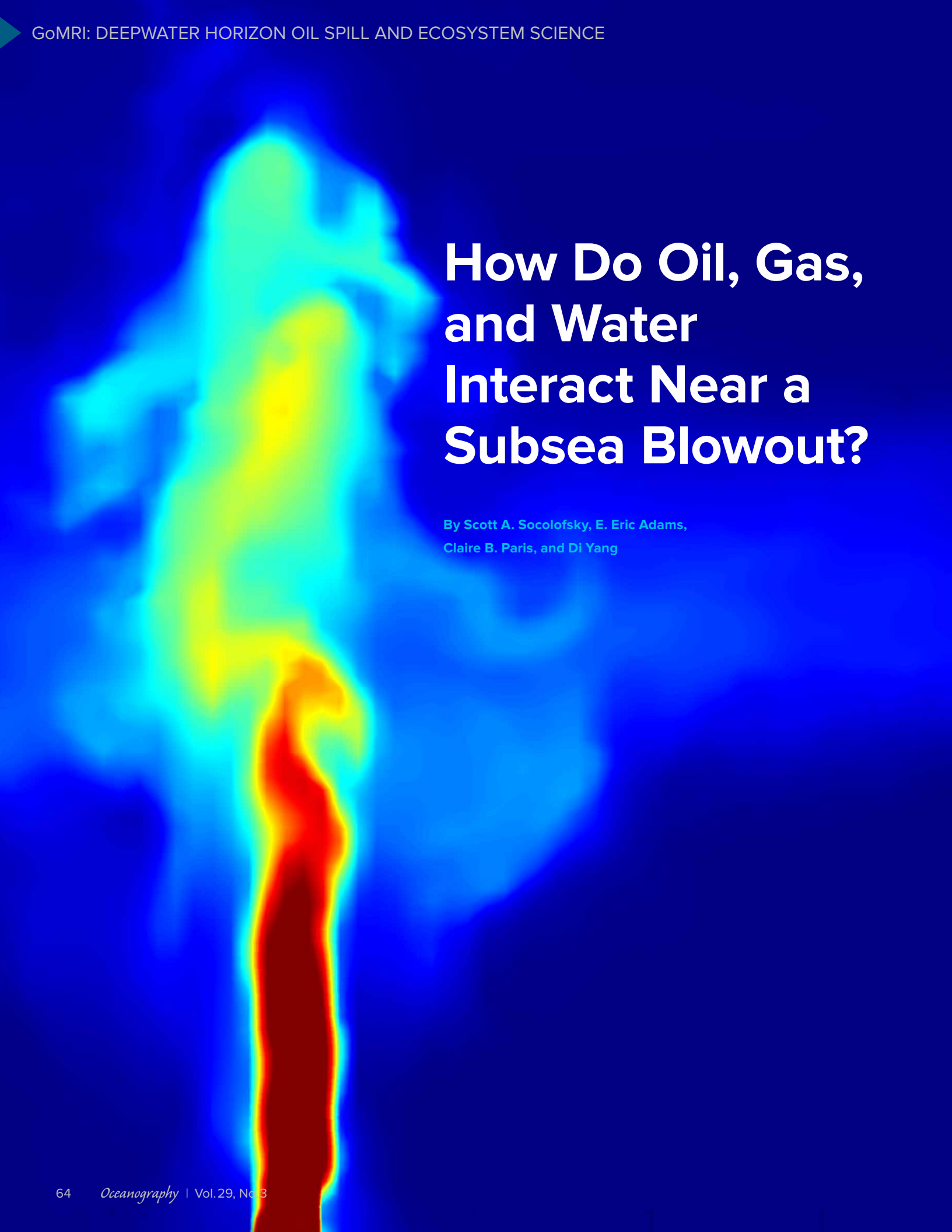
<http://dx.doi.org/10.5670/oceanog.2016.63>

COPYRIGHT

This article has been published in *Oceanography*, Volume 29, Number 3, a quarterly journal of The Oceanography Society. Copyright 2016 by The Oceanography Society. All rights reserved.

USAGE

Permission is granted to copy this article for use in teaching and research. Republication, systematic reproduction, or collective redistribution of any portion of this article by photocopy machine, reposting, or other means is permitted only with the approval of The Oceanography Society. Send all correspondence to: info@tos.org or The Oceanography Society, PO Box 1931, Rockville, MD 20849-1931, USA.



How Do Oil, Gas, and Water Interact Near a Subsea Blowout?

By Scott A. Socolofsky, E. Eric Adams,
Claire B. Paris, and Di Yang

“ At low flow rates into seawater, oil jets are laminar and break up into droplets having nearly uniform diameters... However, for higher flow rates, the jet is turbulent, and the oil becomes atomized into a spectrum of smaller droplets whose diameters decrease with increasing flow rate. ”

ABSTRACT. Oil and gas from a subsea blowout shatter into droplets and bubbles that rise through the water column, entraining ambient seawater and forming a plume. Local density stratification and currents eventually arrest this rising plume, and the entrained water, enriched with dissolved hydrocarbons and some of the smaller oil droplets, forms one or more subsurface intrusion layers. Beyond the plume and intrusion layer(s), droplets and bubbles advect and diffuse by local currents and dissolve and biodegrade as they rise to the surface, where they are transported by wind and waves. These processes occur over a wide range of length scales that preclude simulation by any single model, but separate models of varying complexity are available to handle the different processes. Here, we summarize existing models and point out areas of ongoing and future research.

INTRODUCTION

The Deepwater Horizon (DWH) accident demonstrated in dramatic fashion the wide range of processes that affect oil droplets and gas bubbles released from a subsea blowout. These processes begin with breakup of the blowout jet into small droplets and bubbles, followed by their vertical transport as a buoyant plume, horizontal transport within intrusion layers caused by local density stratification, advection and diffusion by local currents, and additional mixing near the surface due to wind and waves. Simultaneously, dissolution and biodegradation alter the oil and gas mixtures. How these processes occur, their rates, and what management strategies may affect them are important questions as we look to understand the impact of DWH on the Gulf of Mexico and to seek mitigation strategies for potential future oil spills. Here, we discuss our present understanding of, and the ongoing research addressing,

small-scale processes that transport oil and gas near a subsea blowout.

Most observations made during DWH were beyond the 5 km response zone—hence, beyond the region of major droplet/bubble dynamics—and primary observations were of the spill's dissolved signature within the water column (e.g., Valentine, et al., 2010; Kessler, et al., 2011; Du and Kessler, 2012). As in all spills, droplet size distribution is critical to predict the oil's fate and transport. For DWH, significant quantities of chemical dispersants were applied subsurface, directly at the spill source, to promote formation of smaller oil droplets (Brandvik et al., 2013). However, no measurements of bubble or droplet size distributions were made in situ at the source. The few measurements made inside the response zone confirmed the strong plume behavior of the oil and gas jet (Camilli et al., 2011), determined the emission composition (Reddy, et al., 2011), and demonstrated that there

was near complete dissolution of methane, significant dissolution of small hydrocarbon molecules (Ryerson et al., 2011), and near complete oxidation of methane in the water column (Du and Kessler, 2012). These measurements highlight the importance of subsurface processes to hydrocarbon fate, yet there remain significant uncertainties in the processes responsible for these effects.

To bridge this gap, studies of transport processes in the nearfield (where vertical plume rise is significant) and farfield (where bubbles and droplets advect independently) are underway by several groups, many funded by the Gulf of Mexico Research Initiative (GoMRI). To communicate research quickly among this network of colleagues, the Nearfield Modeling Listserv was created (nearfield-modeling@listserv.tamu.edu, moderated by author Socolofsky), and the user group has hosted three workshops. This group identified five areas for study: (1) bubble and droplet generation, (2) plume modeling, (3) intrusion formation and coupling to circulation models, (4) particle tracking models, and (5) bubble and droplet fate modeling (an integrative topic present in each of the previous four areas). Here, we discuss the first four topics and touch on dissolution (topic five), showing how oil and gas mix and are dispersed from a subsea blowout. For farfield transformation, see Tarr et al. (2016, in this issue).

MODELING DEEPWATER BLOWOUTS

Droplet Generation

The sizes of bubbles and droplets generated in a subsea blowout affect hydrocarbon transport and fate in several ways. First, oil and gas are buoyant, causing the hydrocarbons to rise toward the surface as a plume (see section on Nearfield Plume Dynamics, below). Second, depending on their sizes, the droplets and bubbles may separate from the entrained seawater, resulting in different pathways to the surface (see section on Intrusion Layer Formation and Farfield Tracking Models, below). And third, droplets and bubbles provide the surfaces across which hydrocarbon constituents are dissolved into seawater and ultimately degraded. Chemical dispersants, designed to reduce interfacial tension and, thus, droplet size, override this process. The effectiveness of dispersants depends on how much smaller they can make the droplets, and how much differently smaller droplets are transported compared with larger, undispersed droplets. While both droplets and bubbles are important, we focus here on oil droplets.

At low flow rates into seawater, oil jets are laminar and break up into droplets having nearly uniform diameters, comparable to that of the orifice or the maximum stable droplet size, whichever is smaller. However, for higher flow rates, the jet is turbulent, and the oil becomes

atomized into a spectrum of smaller droplets whose diameters decrease with increasing flow rate (Figure 1). The transition from laminar to turbulent jet breakup depends on a Weber number (Tang and Masutani, 2003),

$$We = \frac{\rho U_0^2 D}{\sigma}, \quad (1)$$

where ρ = oil density, U_0 = exit velocity, D = orifice diameter, and σ = interfacial tension. At the time of DWH, no consensus models were available to predict actual droplet sizes in the atomization regime. Under these energetic conditions, turbulent pressure fluctuations cause oil to break up into increasingly smaller droplets until they reach a critical size at which breakup is resisted by interfacial tension (Brandvik et al., 2013). Coalescence due to droplet collision may also play a role. For decades, chemical engineers have studied such processes under equilibrium conditions, and developed correlations of characteristic droplet size with a Weber number, choosing values for U_0 and D appropriate for a stirred reactor (Hinze, 1955). However, except for a short distance of several orifice diameters from the source, oil emanating from a blowout is not in equilibrium, but instead exhibits rapidly decreasing turbulence and droplet concentration along the jet trajectory.

Two basic approaches have been taken to predict droplet size under the dynamic conditions in a jet. The first calibrates

observed median droplet diameters d_{50} , measured in laboratory experiments with oil jetted into seawater (e.g., Brandvik et al., 2013), to the Weber number using the orifice diameter and velocity as length and velocity scales in Equation 1. The simplest equation in this empirical approach is

$$\frac{d_{50}}{D} = A We^{-3/5}, \quad (2)$$

where A is a fitting coefficient. Following Wang and Calabrese (1986), Johansen et al. (2013) modified Equation 2 to account for viscosity (which resists droplet breakup when interfacial tension is reduced due to the use of dispersants). They also accounted for the presence of gas mixed with the oil. For a given oil flow rate and orifice, the gas increases the exit velocity of oil; it also increases the downstream buoyancy of the jet relative to a pure oil jet. Johansen et al. (2013) thus predict median droplet size as a function of a modified Weber number,

$$\frac{d_{50}}{D} = A \left[\frac{We}{1 + BVi(d_{50}/D)} \right]^{-3/5}, \quad (3)$$

where We is now based on U_c = a corrected exit velocity to account for gas and buoyancy, $Vi = \mu U_c / \sigma$, μ = dynamic viscosity of oil, and A and B are empirical coefficients. While the effect of oil viscosity has been well verified by laboratory experiments, the effect of gas has not, partly due to the difficulty in distinguishing gas bubbles



FIGURE 1. Oil droplets discharged into water through a 2 mm diameter nozzle (Tang and Masutani, 2003). From left to right, the jet exit velocities are 0.31, 0.97, 1.41, 2.42, and 5.99 m s⁻¹. As a point of reference, the nozzle outer diameter is 2.5 cm.

from oil droplets when both are present.

Equation 3 predicts mean droplet sizes that agree well with a wide range of laboratory experiments and one small-scale field study—DeepSpill described in Johansen et al. (2003)—and provides a promising method to extrapolate to the scale of a major blowout. Aman et al. (2015) developed a variant of this equation by implicitly assuming equilibrium conditions within the jet, and determining model coefficients using droplet sizes observed with oil stirred in a reactor. The form of their empirical equation is similar, but their fit coefficients give droplets sizes that are two orders of magnitude smaller than those of Johansen et al. (2013). The Johansen equation has been shown to predict reliably against laboratory data and one small field experiment involving jet breakup, but data at large scale are lacking to fully validate either model's predictions.

Empirical equations such as Equations 2 and 3 only predict characteristic droplet sizes (e.g., d_{50}) and must assume a distribution for droplet sizes around the characteristic size. Typically, either a Rosin-Rammler or a lognormal distribution is used (Johansen et al., 2013), with parameters describing the distribution widths taken from laboratory experiments. These models also require specification of the interfacial tension σ . If the oil is untreated, σ should be known, but for oil treated with dispersants, the effectiveness with which the dispersant and oil mix depends on the amount, method, and location of injection, causing uncertainty in the actual interfacial tension and, hence, the predicted droplet size (Brandvik et al., 2013; Socolofsky et al., 2015).

The other basic approach to determine droplet size uses a dynamic (or population) model (Figure 2) to simulate droplet breakup and coalescence as oil encounters time-varying conditions. Notable population models developed for multiphase plumes include VDROPI (Zhao et al., 2014) and Nissanka and Yapa (2016). Both account for effects of

interfacial tension and oil viscosity in resisting breakup and are coupled with nearfield buoyant jet models that compute spatially varying turbulence properties and droplet concentrations. Unlike the empirical equations described above, population models simulate the entire droplet size distribution and suggest that this distribution evolves with distance, a facet beginning to be verified experimentally. As with the correlation equations, both population models agree well with available laboratory and field data, but only after calibration.

Laboratory experiments (Gopalan and Katz, 2010; Nagamine, 2014) show that when chemical dispersants are introduced, additional (latent) breakup occurs far from the jet release due to processes such as tip-streaming and tearing. Nagamine (2014) observed time-varying behavior of droplets held in place using a counter-flowing arrangement. Centimeter-size droplets impregnated with chemical dispersants at dispersant-to-oil ratios (DOR) $> 1:250$ broke into very fine droplets (1–50 μm) within minutes, while similar size droplets with lower DOR remained stable for over a day.

At a recent model intercomparison workshop, modelers compared their predictions of droplet size and transport (Socolofsky et al., 2015). For a spill size approximately one-third that of DWH,

most models predicted droplet sizes of 1–10 mm without dispersants, and 0.1–1 mm if dispersants were uniformly mixed with the oil at a DOR of 1:50, though there was significant variability among predictions. Indeed, remaining questions being addressed with ongoing experiments concern the effects of using live oil (containing dissolved gas) and dependence on temperature and pressure. Moreover, in other spill scenarios with different initial conditions, mechanical breakup may be adequate without the use of dispersants. Nonetheless, for the conditions tested, model predictions generally agree that the use of chemical dispersants reduces both droplet sizes and corresponding droplet rise velocities, resulting in more than a tenfold increase in the downstream length of the surfacing oil footprint—a significant measure of the effectiveness of subsea injection of chemical dispersants.

Nearfield Plume Dynamics

Gas bubbles and oil droplets released from a blowout exert an upward force on the local water column, rising collectively as a buoyant, multiphase plume. The plume entrains ambient seawater, lifting it to higher elevations in the water column. As the plume rises, the gas bubbles and smaller molecules of the oil droplets dissolve into the entrained seawater. This

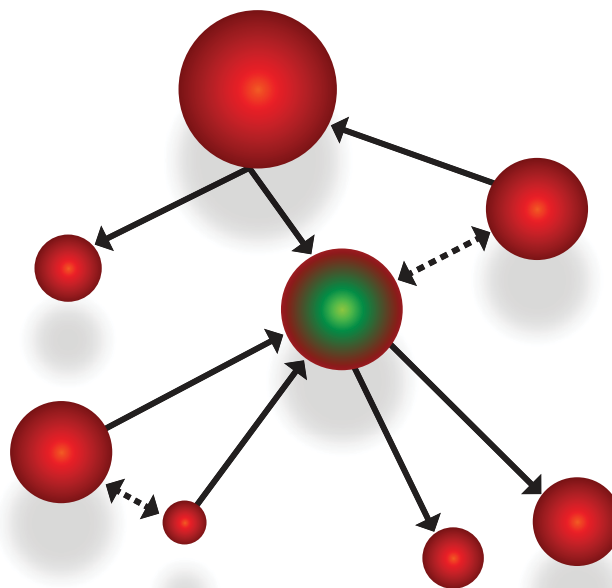


FIGURE 2. Schematic of a dynamic (population) model. The population of droplets of a given size (represented by the red and green droplet in the center) may increase through the breakup of larger droplets or the coalescence of smaller droplets, while the population may decrease through the breakup or coalescence of droplets of the given size.

reduces plume buoyancy as well as bubble and droplet diameters, thereby affecting their rise velocities, and increases the concentration of dissolved hydrocarbons in the plume. Eventually, local density stratification and currents cause the entrained seawater to fall out of the plume, or detrain, forming lateral intrusion layers of enhanced hydrocarbon content, which were observed more than 100 km downstream of the DWH blow-out (Kessler et al., 2011; Du and Kessler, 2012). The plume width and intrusion layer thickness span scales up to a few hundred meters, much smaller than the resolution of ocean circulation models; hence, these features are simulated using submodels specifically designed to capture fine-scale dynamics.

Stratification and crossflow in buoyant multiphase plumes have been studied in the laboratory and in the DeepSpill field experiment. Key parameters controlling their dynamics include: w_r = bubble/droplet rise velocity, B = kinematic buoyancy flux of dispersed phase particles, N = buoyancy frequency of ambient stratification, and u_a = ambient current velocity (Socolofsky and Adams, 2002, 2005). $(BN)^{1/4}$ is a characteristic velocity (Socolofsky and Adams, 2005), and B/w_r^3 gives a characteristic length scale of a multiphase plume (Bombardelli et al., 2007). Combinations of these parameters have been used to predict characteristics of plumes (Figure 3).

Although self-similarity is not strictly valid for multiphase plumes,

integral models based on the entrainment hypothesis have been successfully applied to predict multiphase plume dynamics (Milgram, 1983). Two major blow-out simulation models are DeepBlow (Johansen, 2003) and Clarkson Deep Oil and Gas (CDOG; Zheng and Yapa, 2002). These models have been carefully validated and can predict the dissolution of gas bubbles (Zheng and Yapa, 2002), usually treating oil droplets as inert. They run quickly, making them ideal for response and for exploring sensitivity to complex bubble and droplet behavior and chemistry. Disadvantages are that they cannot resolve unsteady flow features or the complex processes of detrainment, intrusion formation, and weak plume dynamics above the detrainment point.

Recently, large eddy simulation (LES) has been applied to complex oil and gas plumes in stably stratified conditions (Fabregat et al., 2015, and recent work of Alexandre Fabregat, City University of New York, and colleagues; Fraga et al., 2016; Yang et al., 2016). LES models do not rely on self-similarity and are able to directly resolve large- and intermediate-scale turbulent motions, relying on closure models for the effects of subgrid-scale (SGS) features.

These LES models treat water as the continuous phase and bubbles and droplets as dispersed phases. Using an Eulerian framework, the incompressible Navier-Stokes equations are solved for the water velocity field, and a convection-diffusion equation solves for the water density field, which is coupled to the buoyancy term in the Navier-Stokes equations using the Boussinesq approximation (Fabregat et al., 2015; Yang et al., 2016). Both flow and density equations are filtered at the LES grid scale, and several different SGS models have been used to close the equations. For example, Fraga et al. (2016) used the standard Smagorinsky SGS model with a constant coefficient; Fabregat et al. (2015, and recent work of Alexandre Fabregat, City University of New York, and colleagues) employed a spectral vanishing viscosity technique

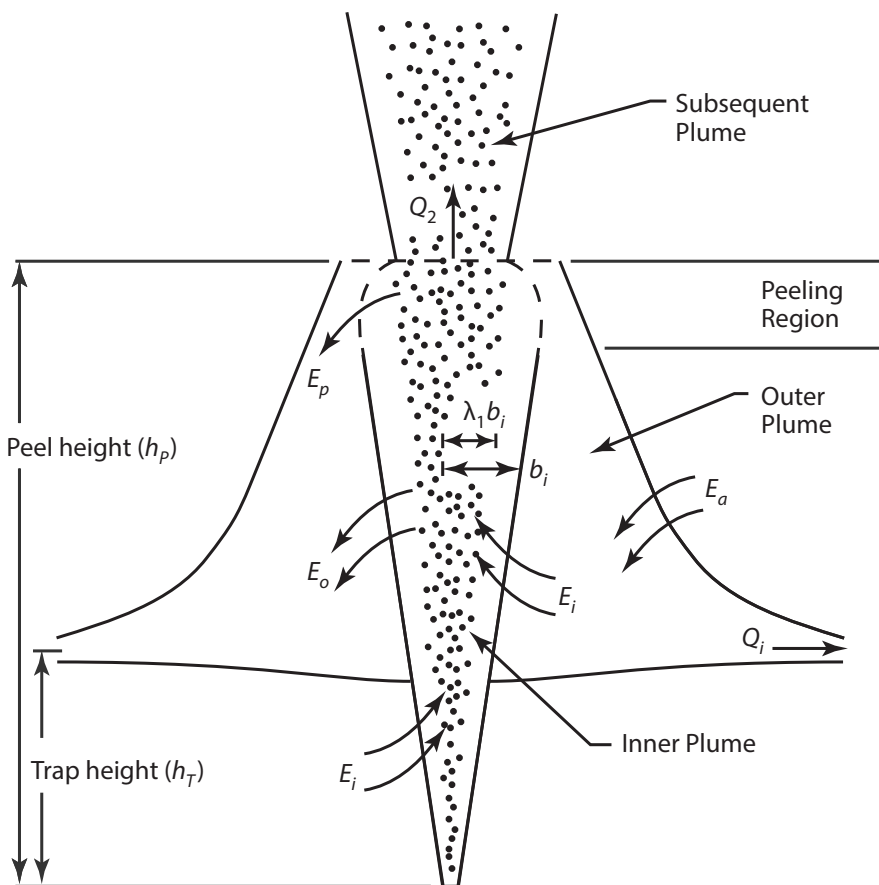


FIGURE 3. Schematic of a multiphase plume discharging to a stratified quiescent water column (after Socolofsky et al., 2008, with permission from ASCE). Bubbles and droplets create a buoyant plume that rises, entraining ambient seawater along the way. At some elevation h_p , the mixture of relatively light bubbles and droplets plus heavy entrained seawater runs out of momentum, and the seawater detrains (peels), ultimately becoming trapped at an elevation h_t where it is neutrally buoyant relative to the ambient seawater. Symbols relate to the double (inner and outer) plume model used to describe this phenomenon.

suitable for their spectral-element code; and Yang et al. (2016) used a Lagrangian-averaged scale-dependent dynamic SGS model developed for complex turbulent flows with spatial inhomogeneity.

Regarding dispersed phases, LES models can be categorized into two approaches. In Fraga et al. (2016), Eulerian-Lagrangian models track the motions of individual particles based on Newton's second law according to forces acting on individual particles. The reaction force from the particles to the fluid is calculated by accounting for

the contributions from all particles in the vicinity of an Eulerian grid point. By contrast, Fabregat et al. (2015, and recent work of Alexandre Fabregat, City University of New York, and colleagues) and Yang et al. (2016) employ Eulerian-Eulerian models, defining a dispersed phase Eulerian concentration, which obeys a convection-diffusion equation.

Using the Eulerian-Eulerian approach, Fabregat et al. (2015, and recent work of Alexandre Fabregat, City University of New York, and colleagues) studied the characteristics of thermal, gas, and

thermal/gas hybrid plumes. By considering varying bubble rise velocities, Yang et al. (2016) systematically studied instantaneous and mean plume characteristics, focusing on the turbulent entrainment, peeling, and intrusion processes (Figure 4a). Yang et al. (2016) also assessed the flux parameterizations typically used in integral plume models. Based on their analysis, they proposed a new continuous peeling model for double-plume integral models with more self-consistent performance than previous models.

A major challenge for both integral

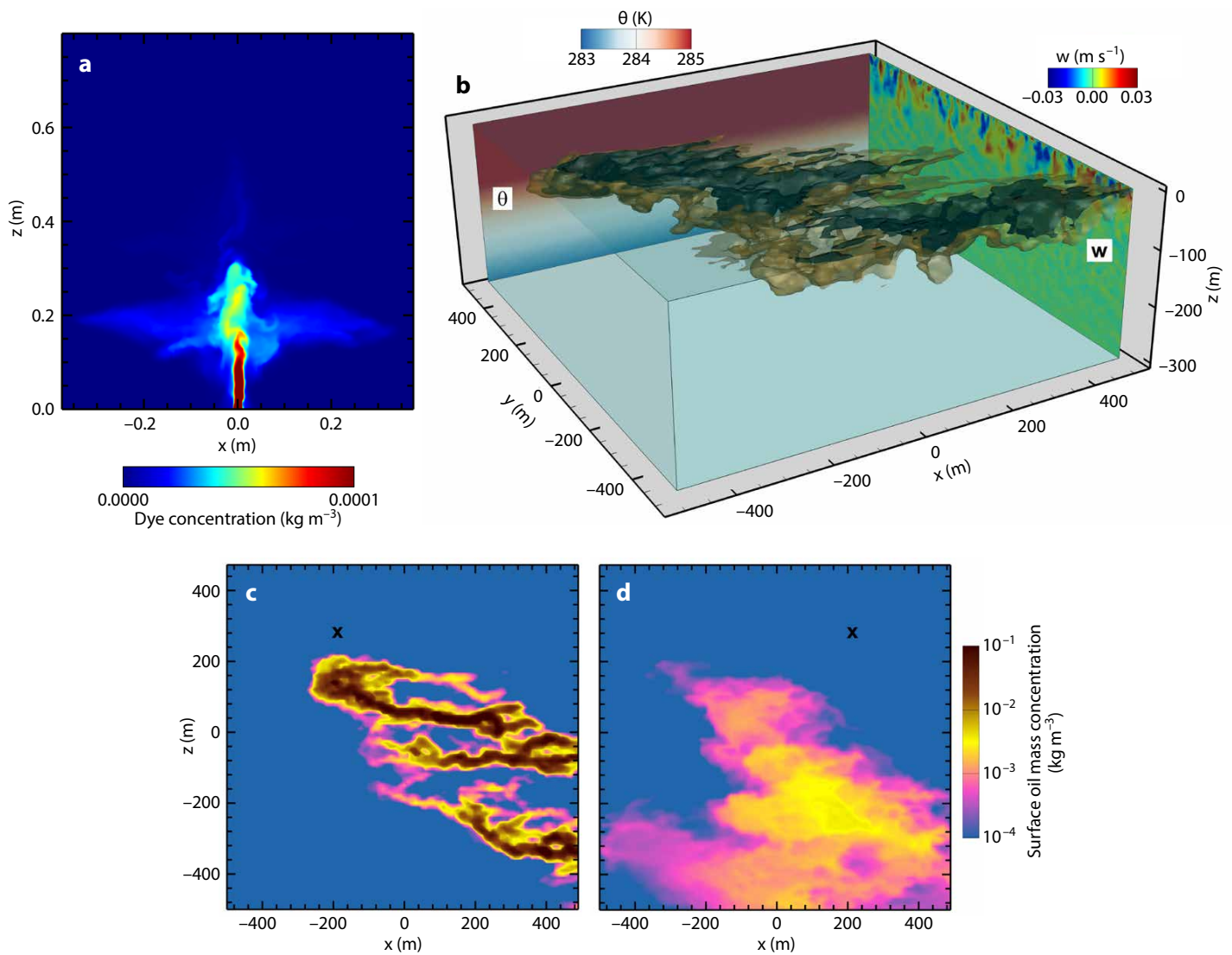


FIGURE 4. Sample results obtained by the Eulerian-Eulerian large eddy simulation (LES) model. (a) Laboratory-scale LES of nearfield plume (corresponding to the case WR6 in Yang et al., 2016), taken after 80 s of simulated bubbling on the x-z plane, across the center of the source, with contours of instantaneous dye concentration. (b-d) Field-scale LES of farfield oil plume dispersion in an ocean mixed layer for a flow condition with Langmuir number $La_t = 0.43$ (corresponding to the flow case L2 in Yang et al., 2015). (b) A plume with oil droplets 250 microns in diameter, with contours of vertical velocity w and temperature θ shown on the two vertical planes at $x = 500$ m and $y = 500$ m, respectively. (c) Surface oil mass concentration (kg m^{-3}) for a plume with 500-micron oil droplets. (d) Surface oil mass concentration (kg m^{-3}) for a plume with 125-micron oil droplets. Details of the simulation setups for the nearfield and farfield LESs can be found in Yang et al. (2016) and Yang et al. (2015), respectively.

and computational fluid dynamics (CFD) models is predicting dissolution of oil droplets and gas bubbles. Dissolution is complicated by the complex chemistry of hydrocarbon mixtures (Chen and Yapa, 2001), including the possible formation of clathrate hydrate skins on the bubbles or droplets. Hydrate formation is pressure- and temperature-dependent, and has recently been studied in high-pressure laboratory facilities (Warzinski et al., 2014) and at natural seeps (B. Wang et al., 2016). In the latter study, in situ high-speed imagery of seep bubbles near 1,000 m depth confirmed the formation of hydrate skins on gas bubbles from natural seeps in the field, and field measurements indicate that mass transfer rates vary between rates for clean and dirty bubbles (Rehder et al., 2009; B. Wang et al., 2016). Mass transfer rates are maintained at the dirty bubble rate (i.e., they are not further reduced by the hydrate skin), likely due to cracks on the hydrate skin, as observed by Warzinski et al. (2014), and the rise height of the seep flares depends on the rise of the largest gas bubbles released from the seep. More measurements are needed to determine the hydrocarbon distribution in the water column, and to understand how the greater turbulent mixing of live oil and gas in a real blowout may differ from that in a weak natural seep flare.

Intrusion Layer Formation

The previous section describes nearfield plume dynamics, showing how buoyant oil and gas, released at the bottom of a stratified ocean, can become trapped in layers, centered on the level of neutral buoyancy of the entrained seawater. It is of interest to know whether oil droplets also become trapped. Experimental studies suggest the classification shown in Figure 5 (Chan et al., 2015), indicating that, as the characteristic velocity $U_N = w_r/(BN)^{1/4}$ decreases, droplets become more effective at pumping ambient water upward to one or more intrusion layers, and there is greater tendency for droplets to detrain and enter the intrusion themselves. Chan et al. (2014) found a threshold value of $U_N = 0.2$ to 0.4, below which droplets intrude. They also derived theoretically and confirmed experimentally a relationship for the distance σ_r that a droplet travels within the first intrusion layer before escaping, given by

$$\sigma_r = \sqrt{\frac{0.9 - 0.38(U_N)^{0.24}}{\pi}} \frac{B^{3/8}}{N^{5/8} W_r^{1/2}} \quad (4)$$

Additional experiments have been conducted to establish similar threshold values of U_N and lateral transport distances for oil discharging into a mild current (Wang and Adams, 2016).

Using Equation 4 for an oil with density of 0.85 g cm^{-3} , droplets with a diameter of 2–20 μm , typical of those expected for untreated oil at DWH (Testa et al., in press), would be transported 50–100 m radially within the intrusion layer. Droplets that are 0.2–2 μm in diameter, typical of those for dispersant treated oil without any latent breakup (Zhao et al., 2015), would travel 100–500 m laterally. Finally, droplets with a diameter of 0.02–0.2 μm , typical of those expected at DWH for dispersant-treated oil experiencing significant latent breakup (Nagamine, 2014) could theoretically be transported 3–20 km before rising out of the intrusion layer. These transport distances are in general agreement with predictions for similar droplet sizes in farfield transport models (Paris et al., 2012; North et al., 2015).

Farfield Tracking Models

We have seen how hydrocarbons from a blowout break up into small oil droplets and gas bubbles, and how these buoyant fluids interact in the nearfield with local ocean currents and stratification to form a plume and intrusion layers. For the farfield, Paris et al. (2013) consider mixing of rising oil droplets and dissolved hydrocarbons, and Lagrangian stochastic models (LSM) can be used to

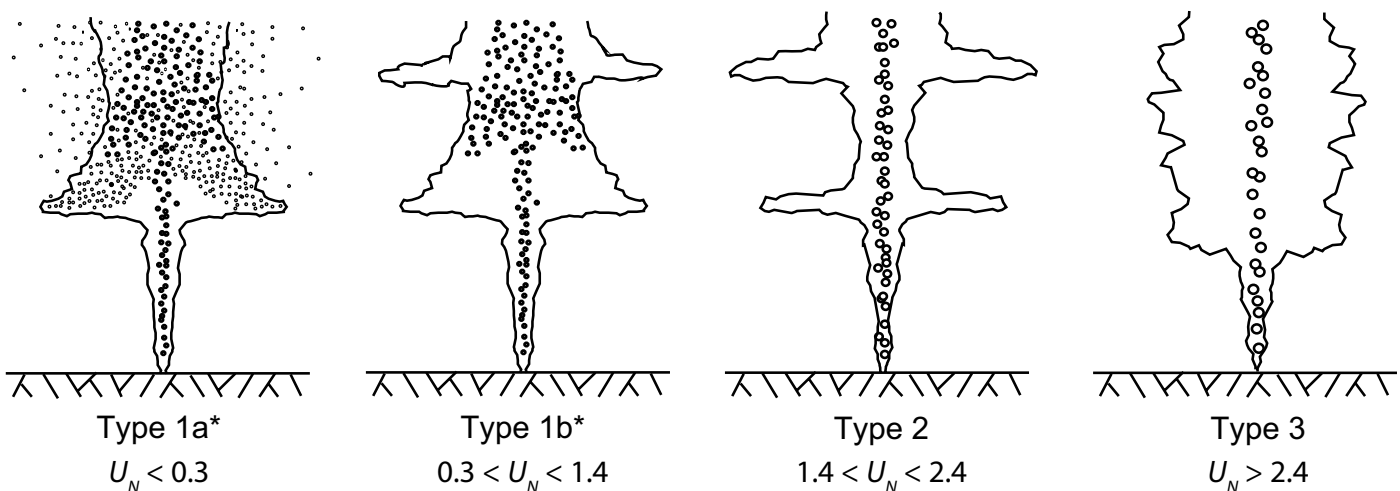


FIGURE 5. Plume classification scheme (after Chan et al., 2015, reproduced with the permission of Springer). The four panels depict droplet plumes with four ranges of dimensionless droplet slip velocity U_N given by the ratio of the droplet rise velocity to a characteristic water velocity in the plume. As U_N decreases, droplets rise more slowly and become more effective at pumping seawater upward. They are also more passive in the plume, and are broadcast more widely in the radial direction.

simulate subsequent fate and transport of multi-fraction Lagrangian elements (Paris et al., 2012; North et al., 2015).

The locations, flow rates, and compositions of oil droplets leaving the intrusion layers become initial conditions for far-field transport models. These inputs can be obtained from integral or LES models of the nearfield, as discussed previously, or from correlation equations, as reported in Socolofsky et al. (2011). In the LSM, particle sizes are typically selected from the droplet size distribution (DSD) at the end of the nearfield, either by binning the data (North et al., 2015) or by a random number generator matched to the DSD probability function (Paris et al., 2012); particle properties, including the density of various hydrocarbon fractions, are matched to the results of the nearfield model.

The boundary conditions specifying the three-dimensional flow field come from ocean circulation models. Currently, the coupling between the near-field plume and ocean circulation models is only in one direction (i.e., the near-field model depends on the farfield flow field but not vice versa). This one-way coupling is also true between the farfield tracking and ocean circulation models. Because the nearfield plume induces significant vertical velocity and the intrusion layer can generate a large flow rate (about $1,000 \text{ m}^3 \text{ s}^{-1}$ for the primary intrusion during DWH), two-way coupling may be important between the buoyancy-dominated near and intermediate field (region of the intrusion formation) and the ocean circulation. The CARTHE and C-IMAGE II consortia are studying this problem, but to date, no two-way coupled hindcast simulations for the near- and farfield of the DWH accident have been reported.

For an LSM, oil is typically represented by Lagrangian elements representing dissolved hydrocarbons or oil droplets with appropriate droplet size and density (Paris et al., 2012; North et al., 2015). These Lagrangian elements are advected by mean ocean currents and droplet rise velocity that varies based on

the temperature and salinity of the ambient water, diffused by ambient turbulence, and transformed by a host of physical, chemical, and biological processes, including dissolution, biodegradation (Lindo-Atichati et al., 2014), high pressure (Aman et al., 2015), and sediment particle interactions (Paris et al., 2012; North et al., 2015). While oil transformations are critical for determining oil fate, we focus here on transport and mixing. For a discussion of transformation, see Tarr et al. (2016, in this issue).

Ocean circulation models, such as SABCOM (used with the transport model LTRANS; North et al., 2015) and GoM-HYCOM (used with the oil application of the Connectivity Modeling System, CMS; Paris et al., 2013) provide the velocity fields, and transport models calculate the local currents by fine-scale interpolation from the CFD gridded velocity. These CFD models generate three-dimensional flow fields over complex bathymetry, often using nested domains that provide added resolution in critical areas, and may respond to tides,

wind, air/sea fluxes, density variations, and Earth's rotation (Coriolis force), among others. Many ocean circulation models also rely on data assimilation to keep model predictions on track.

For tracking of oil droplets, the rise velocity of the droplets, which is dependent on droplet diameter and density (Zheng and Yapa, 2000), is added to the advection predicted from the ocean currents. Because smaller droplets rise more slowly than larger droplets, horizontal currents stretch the spatial distribution

of droplets as they rise through the water column. The smallest droplets surface farthest from the source, and mitigation measures to reduce droplet size (e.g., subsurface dispersant injection) or more energetic breakup regimes can cause the surface expression of the oil to move downstream relative to the unmitigated case (Socolofsky et al., 2015).

The dispersion term used in farfield tracking models is normally taken from the horizontal and vertical turbulent diffusivities computed in the ocean circulation models. These diffusivities can be spatially variable and are treated with random walk algorithms, as in the DWH hindcasts of North et al. (2015) and Paris et al. (2012). Alternatively, model diffusivities can be estimated from field measurements. For example Ledwell et al. (2016) measured concentrations of an introduced tracer (SF_5CF_3) to determine scale-dependent vertical diffusivities, and Z. Wang et al. (2016) used a microstructure profiler to determine small scale turbulent properties, both near the DWH site.

“ The sizes of bubbles and droplets generated in a subsea blowout affect hydrocarbon transport and fate in several ways. ”

One important property affecting particle transport is the turbulent velocity $w_e = \varepsilon^{1/2}/N^{1/2}$, where ε = the turbulent dissipation rate. By comparing w_e with the rise velocity of oil droplets of varying density and diameter, Z. Wang et al. (2016) conclude that droplets larger than 0.4 mm (rise velocity 6 mm s^{-1}) are unlikely to be significantly affected by turbulence, while those smaller than 0.04 mm (rise velocity 0.1 mm s^{-1}) are expected to become so entangled with turbulence that they might be permanently trapped

below the surface.

In addition to contributing to droplet diffusion, turbulence can also alter droplet rise velocity. Bellani and Variano (2012) used a novel underwater imaging technique to compare effects of turbulence on particles and vice versa, focusing on spherical particles (characteristic of small oil droplets) and prolate ellipsoidal particles (characteristic of larger oil droplets). Their results show that smaller droplets are more affected by turbulence, leading to slower rise velocities than in the quiescent case. Current transport models use correlations for terminal rise velocity in quiescent ambient conditions. For large droplets, these correlations are likely acceptable, but for smaller droplets, these correlation equations will predict oil surfacing closer to the source than may actually occur. For response modeling, this behavior is conservative, but for effects modeling and damage assessment, more sophisticated droplet-turbulence

interaction may be warranted.

Figure 6 shows a result from the CMS model for DWH using GoM-HYCOM for the ocean circulation. The figure visualizes the farfield oil distribution by isosurfaces of oil concentration for July 14, 2010, the day the Macondo well was capped. We chose high concentration values to illustrate the complex effects of planetary rotation and bathymetry on hydrocarbons in the water column near the DWH blowout; the full extent of the subsurface distribution of droplets would be seen if lower concentration thresholds were included. The figure shows the anticyclonic behavior of the oil due to planetary rotation in the GoM-HYCOM simulation. Large eddies are captured in the velocity field predicted by HYCOM, illustrating the importance of the underlying circulation model predictions for the farfield tracking models for long-term simulations. Smaller eddies not captured in the circulation model are folded into the

dispersion term in the tracking model. Hence, results for farfield transport models should always be interpreted with respect to the resolution and assumptions in both the underlying ocean circulation model and the coupled Lagrangian tracking model.

Processes in the Surface Mixed Layer

After being subjected to turbulent entrainment and peeling/intrusion processes in the nearfield and lateral transport processes in the farfield, some of the oil droplets finally rise to the very upper portion of the ocean—the ocean mixed layer (OML)—where physical properties of seawater are well mixed. Important flow structures, for example, wind-generated turbulence, surface waves, Stokes drift, Langmuir circulations, and Ekman spirals, often coexist in the OML, causing lateral and vertical dispersion and affecting the oil's surface footprint. Oil

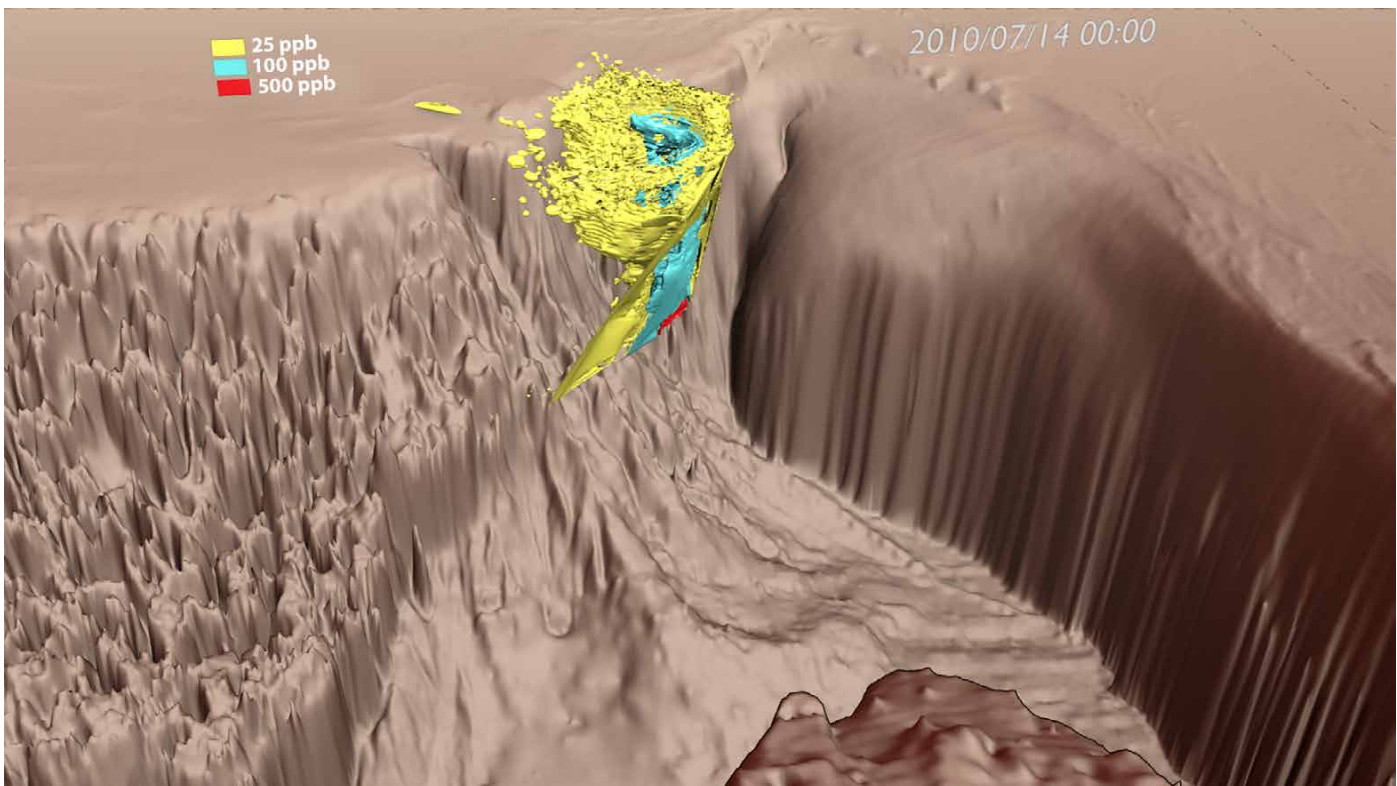


FIGURE 6. Planetary effect on the Deepwater Horizon blowout. Oil structure in the farfield is visualized by the isosurfaces of oil concentration for 550, 110, and 25 ppb on day 85 (July 14, 2010), the day prior to capping of the wellhead. The visualization does not include the nearfield plume. The isosurfaces selected here are for high concentrations to enhance visualization of the anticyclonic rotation; the smaller oil concentrations showing the extent of the spill are not represented here.

reaching the surface from a deep spill will generally form a very thin slick, especially if chemical dispersants have been used. Thus, its subsequent spreading is not amenable to classical analyses applied to surface spills that involve balances of gravity, inertia, viscosity, and surface tension (e.g., Hoult, 1972). Instead, other factors dominate the spreading, including: (1) oil droplets take different pathways to the surface, which increases their surface footprint; (2) wind, waves, and non-uniform currents diffuse and break up the slick; and (3) droplets periodically disperse and resurface, thus tending to stretch the plume, a process likely to increase in significance when considering the fate of chemically dispersed oil. Many of these flow phenomena have characteristic length scales much smaller than the submesoscale, so they are not considered in typical large-scale ocean circulation models used in predicting oil transport (e.g., SABGOM and HYCOM).

Recently, LES-based ocean turbulence models have been used to study fine-scale oceanic flows and their effects on scalar dispersion. Using LES, Yang et al. (2014, 2015) and Chen et al. (2016b) studied oil dispersion in ocean Langmuir turbulence, a flow system that combines the aforementioned fine-scale flow phenomena in the OML. Their LES model solved the filtered Craik–Leibovich equations, which comprise a wave-averaged version of the Navier–Stokes equations but differ from the regular Navier–Stokes equations by inclusion of an extra vortex force term that accounts for the cumulative effects of surface waves on the shear turbulence responsible for generating Langmuir circulations. The intensity of the vortex force can be measured by the turbulent Langmuir number $La_t = \sqrt{u_*}/U_S$, where u_* is the wind-induced friction velocity in the OML and U_S is the magnitude of the Stokes drift. Scalar quantities obey regular transport equations, which include the wave-induced Stokes drift.

Using their LES model, Yang et al. (2014, 2015) studied the complex dispersion of oil plumes in the OML, capturing

simultaneously the effects of Langmuir circulation, turbulence, Stokes drift, and oil droplet buoyancy (Figure 4b–d). Their results reveal that instantaneous oil plume patterns as well as the averaged plume transport direction are affected by two competing mechanisms, downward mixing induced by Langmuir turbulence, characterized by the velocity U_S , and the droplet rise, given by w_r , summarized by the ratio $Db = U_S/w_r$. Plumes with large droplets ($Db < 10$) tend to form fingered patterns, with the mean transport primarily downwind (Figure 4c); plumes with small droplets ($Db > 25$) tend to be highly diffused, with significant crosswind mean transport (Figure 4d); and plumes with intermediate droplets ($10 < Db < 25$) usually have blurred patterns that exhibit surface convergence and form fingered patterns, but with no clean gaps between fingers (Figure 4b).

Based on an extensive set of LES runs, Yang et al. (2015) studied the behavior of eddy viscosity and eddy diffusivity for oil dispersion, and proposed a modified K -profile parameterization (KPP) that incorporates the effects of Langmuir circulations and oil droplet buoyancy into classical KPP. Subsequently, Chen et al. (2016a) also applied the LES model to study the effect of arbitrarily oriented ocean swell waves on the transport and dilution of oil in the OML. They found that when varying the swell-wind relative angle, strong swell waves not only affect the mean transport of the oil plume via the strong swell-induced Stokes drift but they also influence instantaneous oil dilution by modulating the intensity of the turbulence and the Langmuir circulations.

The aforementioned LES studies illustrate the importance of considering fine-scale ocean flow structures in order to accurately predict mean-plume transport and dilution, which are typically not included in regional ocean circulation models due to limited grid resolution. On the other hand, the typical LES domain size of order 1 km is insufficient for tracking long-range plume evolution. To overcome this limit, Chen et al.

(2016b) developed a new approach called the Extended Nonperiodic Domain LES for Scalar transport (ENDLESS), which offers several major advances: (1) It increases the effective LES domain size by solving the flow field on a typical periodic LES domain and tracking the evolution of the nonperiodic oil plume field over a laterally extended domain (replicating the LES velocity field periodically). (2) It efficiently tracks large-scale plume dispersion by adaptively adding and removing simulation blocks for the scalar solver, depending on the real-time spatial extension of the oil plume. (3) It incorporates the numerical capability of superimposing larger-scale quasi-two-dimensional flow motions on oil advection, allowing for coupling with regional circulation models. As the first step, this new ENDLESS model may serve to bridge the gap between traditional LES and large-scale ocean circulation models.

CHALLENGES AND OPPORTUNITIES

Nearfield behavior spans wide spatial scales, from submillimeter droplet-scale processes to advection by ocean currents over hundreds of kilometers, and it depends on intricate multiphase fluid dynamics, chemistry, and biodegradation of complex mixtures at extreme temperatures and pressures. Much success has been achieved through laboratory, field, and numerical experimentation, yet many uncertainties remain. A major challenge affecting the initial condition for transport simulations is that oil droplet breakup occurs at larger We than what can be achieved in laboratory-scale models. Present predictions of droplet size for DWH, for instance, must extrapolate several orders of magnitude beyond the nearest measurement. Because of the importance of droplet size on downstream processes, scaled-up experiments are critically needed.

At the small scale, uncertainties include the sensitivity of model predictions to complex chemical and biological processes. Dissolution and mass transfer

are fundamentally known, and recent data are helping to understand the role of hydrates. However, in computationally expensive models, like LES and the far-field tracking models, expensive chemistry calculations may not be affordable. In this case, it remains to understand the sensitivity of model predictions to these processes and to develop simplified representations of oil fate.

At the large scale, there remains a need to couple the nearfield dynamics with ocean circulation models in order to resolve submesoscale eddies and account for the effect of Earth's rotation. In the case of DWH, the oil mixture released for 86 days was subject to Coriolis forcing, which affected the far-field dynamics (Figure 6). Several studies in the C-IMAGE and CARTHE consortia show the importance of these processes on mixing and flow stability, but integrating these effects with field-scale models remains a challenge. The inexpensive integral models are steady state; hence, they can quickly adapt to changing boundary conditions, but they may not be effective at predicting coupled dynamics. LES models show promise in this area, and the ENDLESS approach described above may yield a working model. But, presently, continued improvement in model resolution and in determining the sensitivity of model predictions to these dynamics is required. Meanwhile, advances in coupled nearfield-farfield dynamic modeling together with the use of real-time, seven-day forecasts of high-resolution ocean circulation (e.g., FKeyS-HYCOM) allow for near-real-time tracking and forecasting of oil dynamics and seem to be the most promising approach for rapid evaluation of blowout predictions to support first-response decisions. 

REFERENCES

- Aman, Z.M., C.B. Paris, E.F. May, M.L. Johns, and D. Lindo-Atichati. 2015. High-pressure visual experimental studies of oil-in-water dispersion droplet size. *Chemical Engineering Science* 127:392–400, <http://dx.doi.org/10.1016/j.ces.2015.01.058>.
- Bellani, G., and E.A. Variano. 2012. Slip velocity of large neutrally buoyant particles in turbulent flows. *New Journal of Physics* 14:25,009–25,009, <http://dx.doi.org/10.1088/1367-2630/14/12/125009>.
- Bombardelli, F.A., G.C. Buscaglia, C.R. Rehmann, L.E. Rincon, and M.H. Garcia. 2007. Modeling and scaling of aeration bubble plumes: A two-phase flow analysis. *Journal of Hydraulic Research* 45(5):617–630, <http://dx.doi.org/10.1080/00221686.2007.9521798>.
- Brandvik, P.J., Ø. Johansen, F. Leirvik, U. Farooq, and P.S. Daling. 2013. Droplet breakup in sub-surface oil releases: Part 1. Experimental study of droplet breakup and effectiveness of dispersant injection. *Marine Pollution Bulletin* 73(1):319–326, <http://dx.doi.org/10.1016/j.marpolbul.2013.05.020>.
- Camilli, R., D. Di Iorio, A. Bowen, C.M. Reddy, A.H. Techet, D.R. Yoerger, L.L. Whitcomb, J.S. Seewald, S.P. Sylva, and J. Fenwick. 2011. Acoustic measurement of the Deepwater Horizon Macondo well flow rate. *Proceedings of the National Academy of Sciences of the United States of America* 109:20,235–20,239, <http://dx.doi.org/10.1073/pnas.1100385108>.
- Chan, G., A. Chow, and E.E. Adams. 2015. Effects of droplet size on intrusion of sub-surface oil spills. *Environmental Fluid Mechanics* 15:959–973, <http://dx.doi.org/10.1007/s10652-014-9389-5>.
- Chen, B., C. Yang, C. Meneveau, and M. Chamecki. 2016a. Effects of swell on transport and dispersion of oil plumes within the ocean mixed layer. *Journal of Geophysical Research-Oceans* 121:3,564–3,578, <http://dx.doi.org/10.1002/2015JC011380>.
- Chen, B., D. Yang, C. Meneveau, and M. Chamecki. 2016b. ENDLESS: An extended nonperiod domain large-eddy simulation approach for scalar plumes. *Ocean Modelling* 101:121–132, <http://dx.doi.org/10.1016/j.ocemod.2016.04.003>.
- Chen, F.H., and P.D. Yapa. 2001. Estimating hydrate formation and decomposition of gases released in a deepwater ocean plume. *Journal of Marine Systems* 30:21–32, [http://dx.doi.org/10.1016/S0924-7963\(01\)00032-X](http://dx.doi.org/10.1016/S0924-7963(01)00032-X).
- Du, M.R., and J.D. Kessler. 2012. Assessment of the spatial and temporal variability of bulk hydrocarbon respiration following the Deepwater Horizon oil spill. *Environmental Science & Technology* 46(19):10,499–10,507, <http://dx.doi.org/10.1021/es301363k>.
- Fabregat, A., W.K. Dewar, T. Özgökmen, and A.C. Poje. 2015. Numerical simulations of turbulent thermal, bubble and hybrid plumes. *Ocean Modelling* 90:16–28, <http://dx.doi.org/10.1016/j.ocemod.2015.03.007>.
- Fraga, B., T. Stoesser, C.C.K. Lai, and S.A. Socolofsky. 2016. A LES-based Eulerian–Lagrangian approach to predict the dynamics of bubble plumes. *Ocean Modelling* 9,727–9,736, <http://dx.doi.org/10.1016/j.ocemod.2015.11.005>.
- Gopalan, B., and J. Katz. 2010. Turbulent shearing of crude oil mixed with dispersants generates long microthreads and microdroplets. *Physical Review Letters* 104, 054501, <http://dx.doi.org/10.1103/PhysRevLett.104.054501>.
- Hinze, J.O. 1955. Fundamentals of the hydrodynamic mechanism of splitting in dispersion processes. *AIChE Journal* 1(3):289–295, <http://dx.doi.org/10.1002/aic.690010303>.
- Hoult, D.P. 1972. Oil spreading on the sea. *Annual Review of Fluid Mechanics* 4:341–367, <http://dx.doi.org/10.1146/annurev.fl.04.010172.002013>.
- Johansen, Ø. 2003. Development and verification of deep-water blowout models. *Marine Pollution Bulletin* 47:360–368, [http://dx.doi.org/10.1016/S0025-326X\(03\)00202-9](http://dx.doi.org/10.1016/S0025-326X(03)00202-9).
- Johansen, Ø., P.J. Brandvik, and U. Farooq. 2013. Droplet breakup in subsea oil releases: Part 2. Predictions of droplet size distributions with and without injection of chemical dispersants. *Marine Pollution Bulletin* 73(1):327–335, <http://dx.doi.org/10.1016/j.marpolbul.2013.04.012>.
- Johansen, Ø., H. Rye, and C. Cooper. 2003. DeepSpill: Field study of a simulated oil and gas blowout in deep water. *Spill Science & Technology Bulletin* 8:433–443, [http://dx.doi.org/10.1016/S1353-2561\(02\)00123-8](http://dx.doi.org/10.1016/S1353-2561(02)00123-8).
- Kessler, J.D., D.L. Valentine, M.C. Redmond, M. Du, E.W. Chan, S.D. Mendes, E.W. Quiroz, C.J. Villanueva, S.S. Shusta, L.M. Werra, and others. 2011. A persistent oxygen anomaly reveals the fate of spilled methane in the deep Gulf of Mexico. *Science* 331:312–315, <http://dx.doi.org/10.1126/science.1199697>.
- Ledwell, J.R., R. He, S.F. DiMarco, L. Spencer, and P. Chapman. 2016. Dispersion of a tracer in the deep Gulf of Mexico. *Journal of Geophysical Research* 121:1,110–1,132, <http://dx.doi.org/10.1002/2015JC011405>.
- Lindo-Atichati, D., C.B. Paris, M. Le Hénaff, M. Schedler, A.G. Valladares Juárez, and R. Müller. 2014. Simulating the effects of droplet size, high-pressure biodegradation, and variable flow rate on the subsea evolution of deep plumes from the Macondo blowout. *Deep Sea Research Part II* 129:301–310, <http://dx.doi.org/10.1016/j.dsr2.2014.01.011>.
- Milgram, J.H. 1983. Mean flow in round bubble plumes. *Journal of Fluid Mechanics* 133:345–376, <http://dx.doi.org/10.1017/S0022112083001950>.
- Nagamine, S.I. 2014. *The effects of chemical dispersants on buoyant oil droplets*. MSc Thesis, Department of Mechanical Engineering, University of Hawaii at Manoa.
- Nissanka, I.D., and P.D. Yapa. 2016. Calculation of oil droplet size distribution in an underwater oil well blowout. *Journal of Hydraulic Research* 54(3):307–320, <http://dx.doi.org/10.1080/00221686.2016.1144656>.
- North, E.W., E.E. Adams, A.E. Thessen, Z. Schlag, R. He, S.A. Socolofsky, S.M. Masutani, and S.D. Peckham. 2015. The influence of droplet size and biodegradation on the transport of subsurface oil droplets during the Deepwater Horizon spill: A model sensitivity study. *Environmental Research Letters* 10(2), 024016, <http://dx.doi.org/10.1088/1748-9326/10/2/024016>.
- Paris, C.B., J. Helgers, E. van Sebille, and A. Srinivasan. 2013. Connectivity Modeling System: A probabilistic modeling tool for the multi-scale tracking of biotic and abiotic variability in the ocean. *Environmental Modelling & Software* 42:47–54, <http://dx.doi.org/10.1016/j.envsoft.2012.12.006>.
- Paris, C.B., M.L. Hénaff, Z.M. Aman, A. Subramaniam, J. Helgers, D.-P. Wang, V.H. Kourafalou, and A. Srinivasan. 2012. Evolution of the Macondo well blowout: Simulating the effects of the circulation and synthetic dispersants on the sub-sea oil transport. *Environmental Science & Technology* 46:13,293–13,302, <http://dx.doi.org/10.1021/es303197h>.
- Reddy, C.M., J.S. Arey, J.S. Seewald, S.P. Sylva, K.L. Lemkau, R.K. Nelson, C.A. Carmichael, C.P. McIntyre, J. Fenwick, G.T. Ventura, and others. 2011. Composition and fate of gas and oil released to the water column during the Deepwater Horizon oil spill. *Proceedings of the National Academy of Sciences of the United States of America* 109:20,229–20,234, <http://dx.doi.org/10.1073/pnas.1101242108>.
- Rehder, G., I. Leifer, P.G. Brewer, G. Friederich, and E.T. Peltzer. 2009. Controls on methane bubble dissolution inside and outside the hydrate stability field from open ocean field experiments and numerical modeling. *Marine Chemistry* 114:19–30, <http://dx.doi.org/10.1016/j.marchem.2009.03.004>.
- Ryerson, T.B., K.C. Aikin, W.M. Angevine, E.L. Atlas, D.R. Blake, C.A. Brock, F.C. Fehsenfeld, R.-S. Gao, J.A. de Gouw, D. Fahey, and others.

2011. Atmospheric emissions from the Deepwater Horizon spill constrain air-water partitioning, hydrocarbon fate, and leak rate. *Geophysical Research Letters* 38, L07803, <http://dx.doi.org/10.1029/2011GL046726>.
- Socolofsky, S.A., and E.E. Adams. 2002. Multi-phase plumes in uniform and stratified crossflow. *Journal of Hydraulic Research* 40(6), 661–672, <http://dx.doi.org/10.1080/00221680209499913>.
- Socolofsky, S.A., and E.E. Adams. 2005. Role of slip velocity in the behavior of stratified multiphase plumes. *Journal of Hydraulic Engineering* 131(4):273–282, [http://dx.doi.org/10.1061/\(ASCE\)0733-9429\(2005\)131:4\(273\)](http://dx.doi.org/10.1061/(ASCE)0733-9429(2005)131:4(273)).
- Socolofsky, S.A., E.E. Adams, M.C. Boufadel, Z.M. Aman, Ø. Johansen, W.J. Konkel, D. Lindo, M.N. Madsen, E.W. North, C.B. Paris, and others. 2015. Intercomparison of oil spill prediction models for accidental blowout scenarios with and without subsea chemical dispersant injection. *Marine Pollution Bulletin* 96(1–2):110–126, <http://dx.doi.org/10.1016/j.marpolbul.2015.05.039>.
- Socolofsky, S.A., E.E. Adams, and C.R. Sherwood. 2011. Formation dynamics of subsurface hydrocarbon intrusions following the Deepwater Horizon blowout. *Geophysical Research Letters* 38, L09602, <http://dx.doi.org/10.1029/2011GL047174>.
- Socolofsky, S.A., T. Bhaumik, and D.-G. Seol. 2008. Double-plume integral models for near-field mixing in multiphase plumes. *Journal of Hydraulic Engineering* 134(6):772–783, [http://dx.doi.org/10.1061/\(ASCE\)0733-9429\(2008\)134:6\(772\)](http://dx.doi.org/10.1061/(ASCE)0733-9429(2008)134:6(772)).
- Tang, L., and S.M. Masutani. 2003. Laminar and turbulent flow liquid-liquid jet instability and breakup. Paper presented at the *Thirteenth International Offshore and Polar Engineering Conference*, May 25–30, 2003, Honolulu, HI.
- Tarr, M.A., P. Zito, E.B. Overton, G.M. Olson, P.L. Adhikari, and C.M. Reddy. 2016. Weathering of oil spilled in the marine environment. *Oceanography* 29(3):126–135, <http://dx.doi.org/10.5670/oceanog.2016.77>.
- Testa, J., E.E. Adams, E.W. North, and R. He. In press. Estimating the influence of deep water application of dispersants on the surface expression of oil using a particle tracking model. *Journal of Geophysical Research*.
- Valentine, D.L., J.D. Kessler, M.C. Redmond, S.D. Mendes, M.B. Heintz, C. Farwell, L. Hu, F.S. Kinnaman, S. Yvon-Lewis, M.R. Du, and others. 2010. Propane respiration jump-starts microbial response to a deep oil spill. *Science* 330:208–211, <http://dx.doi.org/10.1126/science.1196830>.
- Wang, B., S.A. Socolofsky, J.A. Breier, and J.S. Seewald. 2016. Observations of bubbles in natural seep flares at MC 118 and GC 600 using in situ quantitative imaging. *Journal of Geophysical Research* 121(4):2,203–2,230, <http://dx.doi.org/10.1002/2015JC011452>.
- Wang, C.Y., and R.V. Calabrese. 1986. Drop breakup in turbulent stirred-tank contactors: Part II. Relative influence of viscosity and interfacial tension. *AIChE Journal* 32(4):667–676, <http://dx.doi.org/10.1002/aic.690320417>.
- Wang, D., and E.E. Adams. 2016. Intrusion dynamics of particle plumes in stratified water with weak crossflow: Application to deep ocean blowouts. *Journal of Geophysical Research* 121, <http://dx.doi.org/10.1002/2015JC011324>.
- Wang, Z., S.F. DiMarco, and S.A. Socolofsky. 2016. Turbulence measurements in the northern Gulf of Mexico: Application to the Deepwater Horizon oil spill on droplet dynamics. *Deep Sea Research Part I* 109:40–50, <http://dx.doi.org/10.1016/j.dsr.2015.12.013>.
- Warzinski, R.P., R. Lynn, I. Haljasmaa, I. Leifer, F. Shaffer, B.J. Anderson, and J.S. Levine. 2014. Dynamic morphology of gas hydrate on a methane bubble in water: Observations and new insights for hydrate film models. *Geophysical Research Letters* 41:6,841–6,847, <http://dx.doi.org/10.1002/2014GL061665>.
- Yang, D., M. Chamecki, and C. Meneveau. 2014. Inhibition of oil plume dilution in Langmuir ocean circulation. *Geophysical Research Letters* 41(5):1,632–1,638, <http://dx.doi.org/10.1002/2014GL059284>.
- Yang, D., B. Chen, M. Chamecki, and C. Meneveau. 2015. Oil plumes and dispersion in Langmuir, upper-ocean turbulence: Large-eddy simulations and K-profile parameterization. *Journal of Geophysical Research* 120(7):4,729–4,759, <http://dx.doi.org/10.1002/2014JC010542>.
- Yang, D., B. Chen, S.A. Socolofsky, M. Chamecki, and C. Meneveau. 2016. Large-eddy simulation and parameterization of buoyant plume dynamics in stratified flow. *Journal of Fluid Mechanics* 794:798–833, <http://dx.doi.org/10.1017/jfm.2016.191>.
- Zhao, L., M.C. Boufadel, E.E. Adams, S.A. Socolofsky, T. King, K. Lee, and T. Nedwed. 2015. Simulation of scenarios of oil droplet formation from the Deepwater Horizon blowout. *Marine Pollution Bulletin* 101(1):304–319, <http://dx.doi.org/10.1016/j.marpolbul.2015.10.068>.
- Zhao, L., M.C. Boufadel, S.A. Socolofsky, E. Adams, T. King, and K. Lee. 2014. Evolution of droplets in subsea oil and gas blowouts: Development and validation of the numerical model VDRO-P-J. *Marine Pollution Bulletin* 83(1):58–69, <http://dx.doi.org/10.1016/j.marpolbul.2014.04.020>.
- Zheng, L., and P.D. Yapa. 2000. Buoyant velocity of spherical and nonspherical bubbles/droplets. *Journal of Hydraulic Engineering* 126(11):852–854, [http://dx.doi.org/10.1061/\(ASCE\)0733-9429\(2000\)126:11\(852\)](http://dx.doi.org/10.1061/(ASCE)0733-9429(2000)126:11(852)).
- Zheng, L., and P.D. Yapa. 2002. Modeling gas dissolution in deepwater oil/gas spills. *Journal of Marine Systems* 31(4):299–309, [http://dx.doi.org/10.1016/S0924-7963\(01\)00067-7](http://dx.doi.org/10.1016/S0924-7963(01)00067-7).

ACKNOWLEDGMENTS

This work was made possible by a grant from the Gulf of Mexico Research Initiative to the Gulf Integrated Spill Research (GISR) Consortium to the Center for Integrated Modeling and Analysis of the Gulf Ecosystem (C-IMAGE I and II), and to the RFP-II project Large Eddy Simulation of Turbulent Dispersion of Oil in the Ocean Surface Layers: Development, Testing, and Applications of Subgrid-Scale Parameterizations.

AUTHORS

Scott A. Socolofsky (socolofs@tamu.edu) is Professor, Zachry Department of Civil Engineering, Texas A&M University, College Station, TX, USA. **E. Eric Adams** is Senior Lecturer and Senior Research Engineer, Department of Civil and Environmental Engineering, Massachusetts Institute of Technology, Cambridge, MA, USA. **Claire B. Paris** is Associate Professor of Ocean Sciences, Rosenstiel School of Marine & Atmospheric Science, Miami, FL, USA. **Di Yang** is Assistant Professor, Department of Mechanical Engineering, University of Houston, Houston, TX, USA.

ARTICLE CITATION

Socolofsky, S.A., E.E. Adams, C.B. Paris, and D. Yang. 2016. How do oil, gas, and water interact near a subsea blowout? *Oceanography* 29(3):64–75, <http://dx.doi.org/10.5670/oceanog.2016.63>.